2D Resistivity imaging of an urban site across from Princess Noura University, Riyadh, Saudi Arabia

Prepared by:

Ahmed Almehisini

Academic supervisor:

Dr. Sattam Almadani

Department of Geology and Geophysics

College of Science - King Saud University

Riyadh, Saudi Arabia

Rajab, 1436 A.H.

May, 2015 A.D.

TABLE OF CONTENTS

Introduction:

The expansion of resistivity surveying methods has been incredibly fast in the most recent three decades. The initiation of computerized data acquisition systems, inversion codes, and simple access to great and rapid computers has extremely amplified the realistic applicability of the geophysical method. Geoelectrical resistivity imaging is more and more being used in environmental, engineering and hydrological investigations as well as geothermal and mineral prospecting, where detailed knowledge of the subsurface is wanted. The use of geoelectrical resistivity surveys for investigating subsurface layered media has its origin in (1912) due to the work of Conrad Schlumberger who conducted the first geoelectrical resistivity experiment in the fields of Normandy; and about (1915), a similar idea was developed by Frank Wenner in the United State of American (USA) (Kunetz, 1966 and Aizebeokhai, 2010). Ever since, geoelectrical resistivity surveying has greatly improved, and has become an important and useful tool in hydrogeological studies, mineral prospecting and mining, as well as in environmental and engineering applications (e.g. Griffithset al., 1990; Griffiths and Barker, 1993; Dahlin and Loke,1998; Olayinka, 1999; Olayinka and Yaramanci, 1999; Amidu and Olayinka, 2006; Aizebeokhai et al., 2010)

Study area:

The 2-D ERT data have been acquired along one profile in a cavity affected area, opposite to the Princess Noura University, Riyadh (Figure 1). The studied site is covered with the Arab Formation that composed Jubaila is consensual and appears on the surface in the form of a slide presentation about (10) km, extends toward the north northwest-south-southeast. This formation forms a distinct layer beneath the city of Riyadh, and by the underground water has melted layers of anhydrite and remain permanently exist. As a result, it has cracked limestone layers and eclipsed collapsed and became structures and fixtures inside this all reflects the impact of this distortion and the possible fragmentation of the formed into three groups, from the bottom limestone rocks calcareous minute crystals in the middle range of breccia (rock composed of fragments coherent angle) in the top limestone rocks minute crystals.

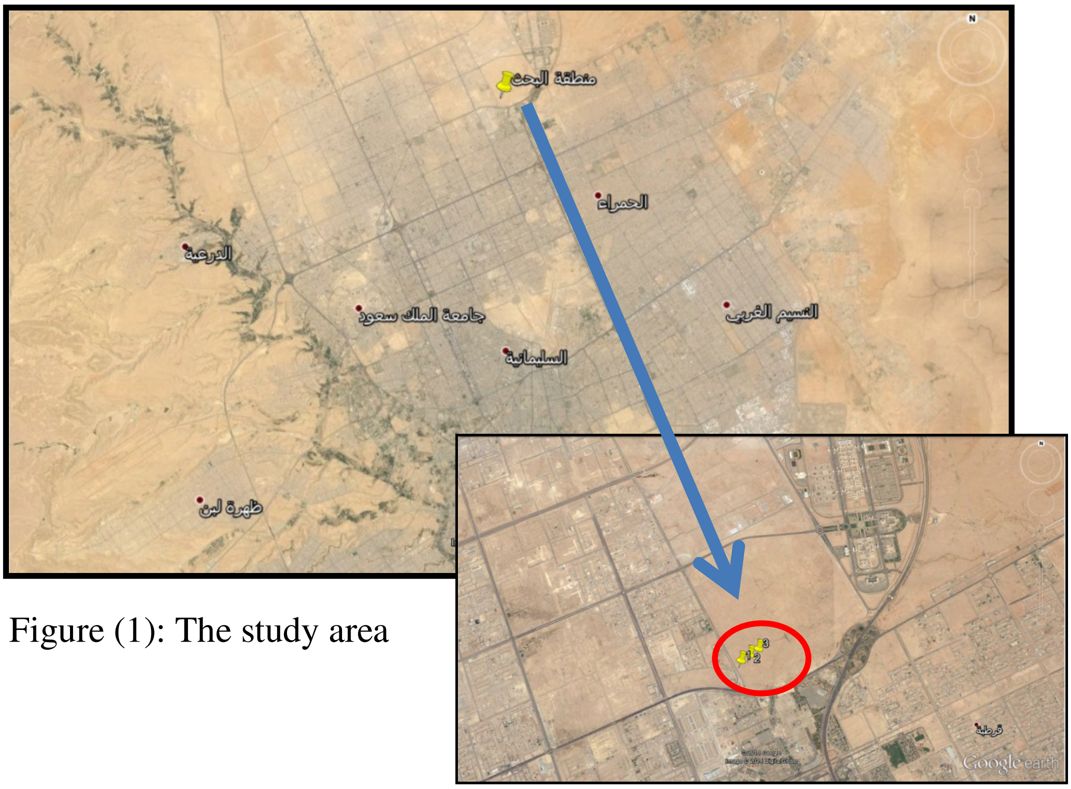

Figure (1): The study area

Theory of 2D resistivity:

The 2D resistivity measurements are normally made by injecting current into the ground through two current electrodes, C1 and C2 and measuring the resulting voltage difference at two potential electrodes, P1 and P2 (Figure 2). The resistivity of a soil or rock is dependent on several factors that include amount of interconnected pore water, porosity, amount of total dissolved solid such as salts and mineral composition (clays).

2D resistivity data acquisition and field survey:

The 2-D ERT data have been acquired along one profile in a cavity affected area, across from to the Princess Noura University, Riyadh (Figure 1). The survey was carried out using Syscal–Pro system (IRIS instruments) with (72) multi-electrodes system, with 18 electrodes cables with (5) m electrode spacing were arranged along a profile. The multi-electrodes were performed using Dipole-Dipole configuration (Figure 2).

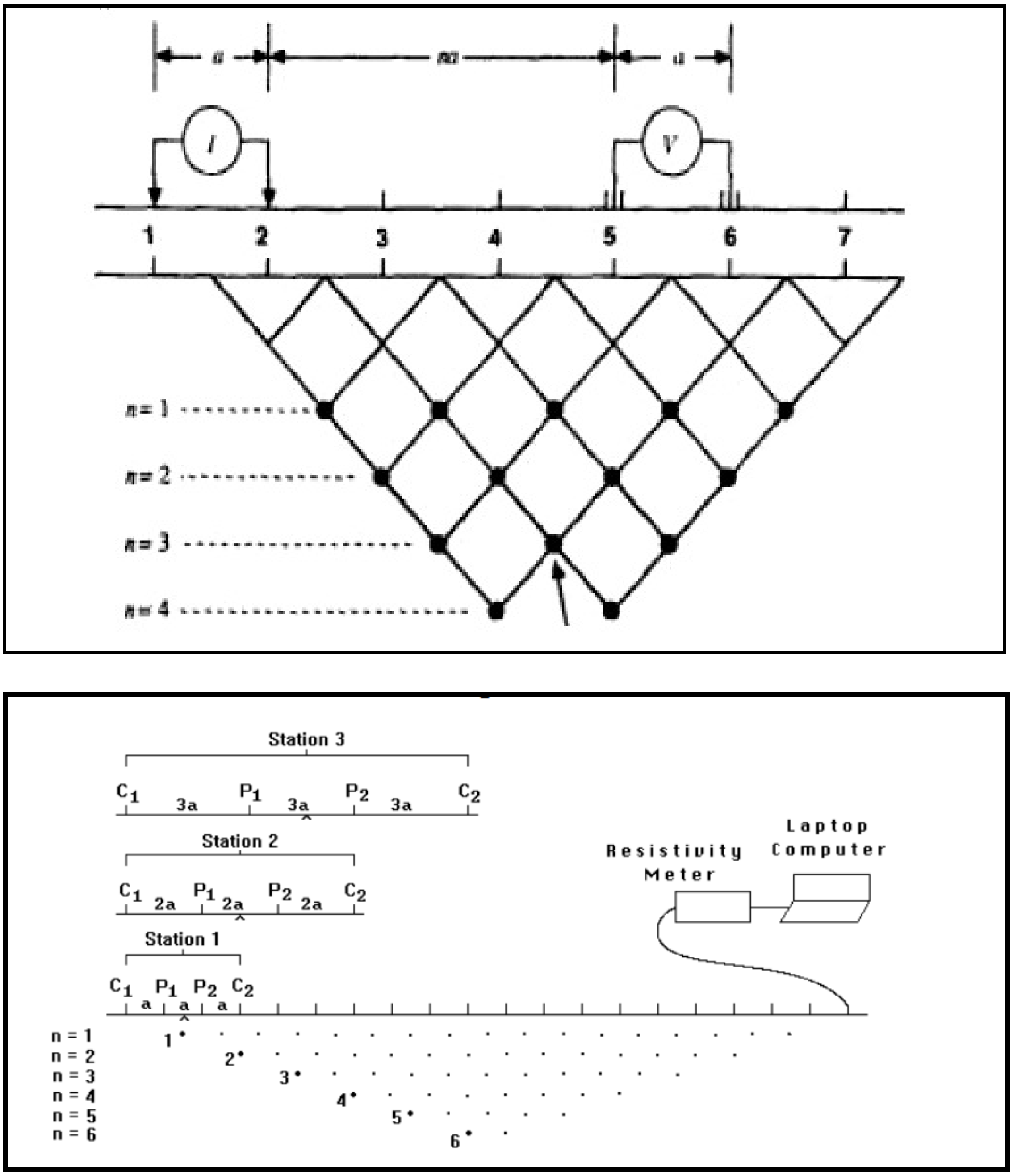

Figure (2): Sequence of measurements to build a pseudo-section using a computer controlled multi-electrodes survey setup.

Figure (3): Field measurements: Inserting electrodes and connecting the measurement system.

Before the starting the field work and data acquisition process, the ELECTRE Pro software is used for creating some 2D surface sequences of measurement for IRIS Instruments SYSCAL Pro-Switch resistivity-meters. The creation of a sequence is made in (3) steps:

1- Creation of the grid ("Creation" tab) depending on:

- Organization of the electrodes
- Number of electrodes
- Positions of the electrodes

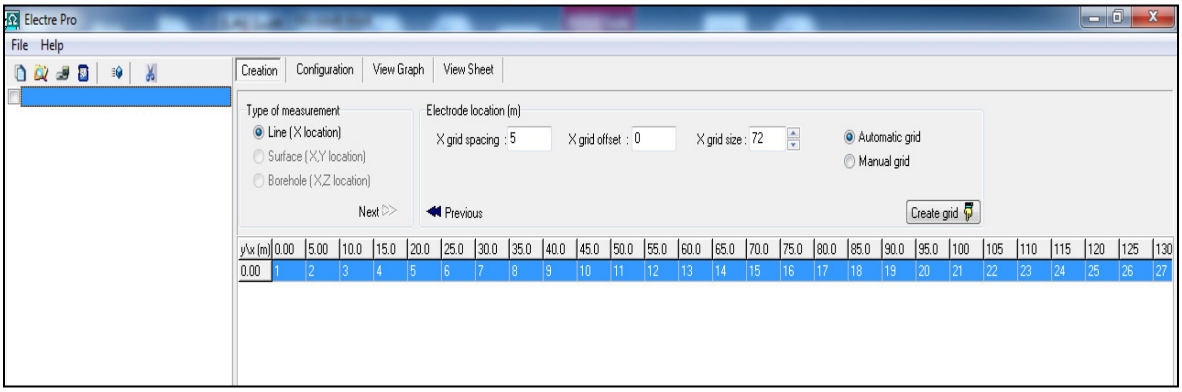

Figure (4): Creation of the survey grid using Electro Pro software.

2- Definition of the parameters of the

- Sequence ("Configuration" tab):
- Timing / quality control
- Electrode array
- Levels of investigation

3- The different spacing and number of depth levels are set graphically as follow:

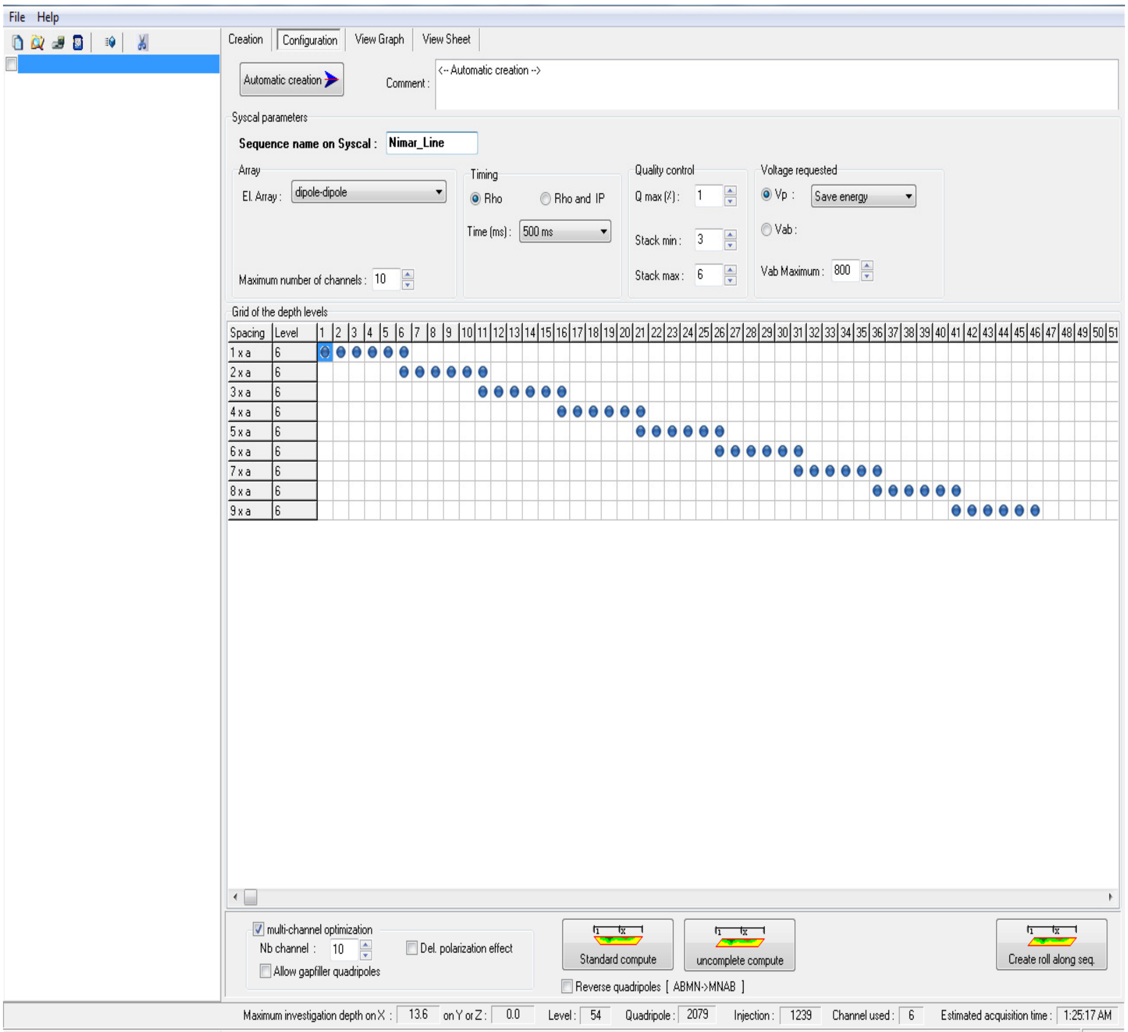

Figure (5): The different spacing and number of depth levels are set graphically as shown using Electro Pro software.

4- The sequence(s) can be then visualized graphically (″View Graph″ tab) or numerically (″View sheet″ tab). A graphical picturing of the created sequence(s) is done so as to visualize the distribution of the data points that will be measured.

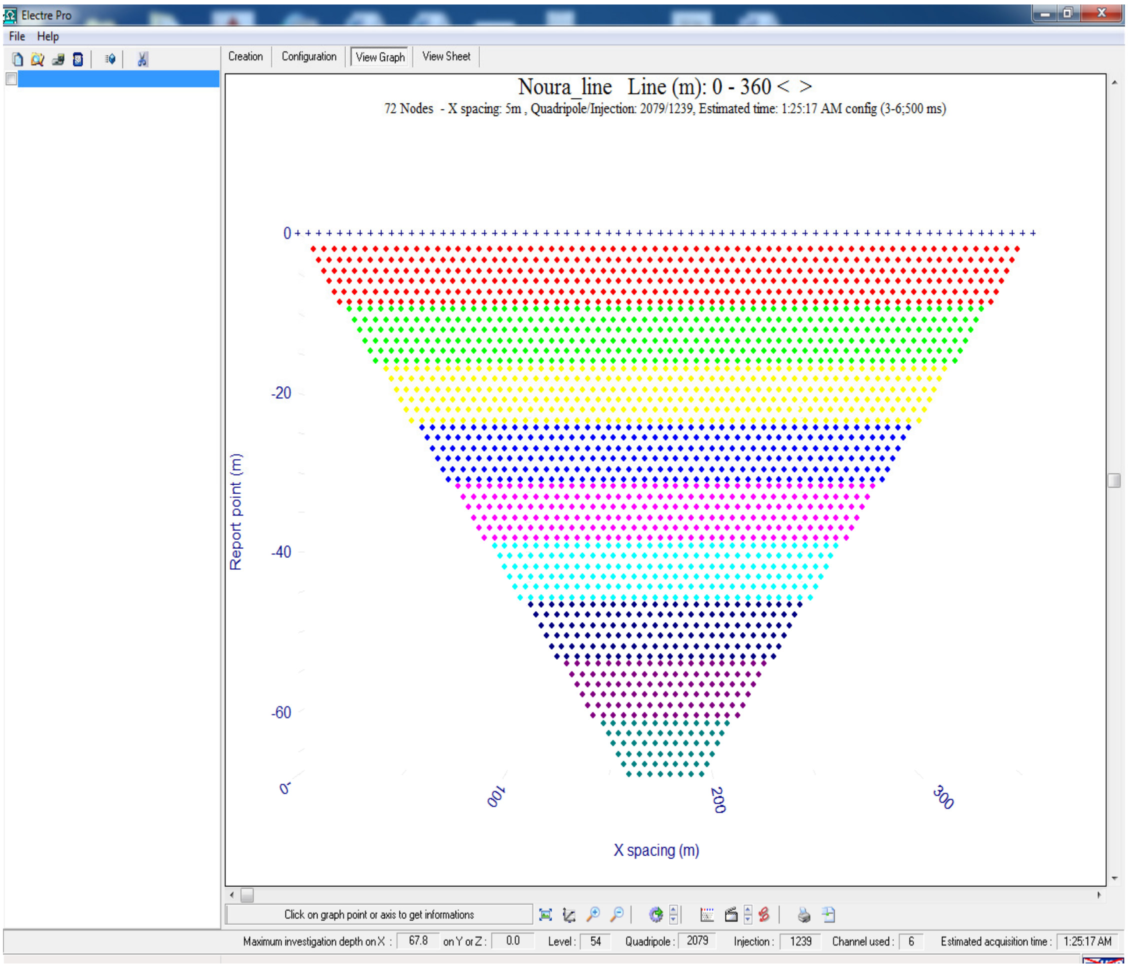

Figure (6): A graphical picturing of the created sequence(s) is done so as to visualize the distribution of the data points that will be measured.

Data download and error elimination:

Before the inversion process, to obtain a true model representing continuous distribution of calculated electrical resistivity in the subsurface, the data were imported to PROSYS II software and the noise and spiky values were edited and eliminated. This step is considered as a prerequisite process step for the next inversion procedure using RES2DINV software, which is based on the regularized least-squares optimization method. The main functions of the PROSYS II software are the following ones:

- Data download
- Numeric and graphic presentation (raw parameters, resistivity, chargeability, …)
- Processing (filter on threshold values, apply a sliding or median average, reject a node, reject the gapfiller quadripoles, create a batch file with a specific filtering to apply to a set of files, …)
- Topography insertion
- Plot of the apparent resistivity and chargeability sections
- Export to various formats (″txt″, Res2dinv, …) and visualization of the exported files.

Step (1): Automatic filtering to eliminate zero and enormous resistivity values:

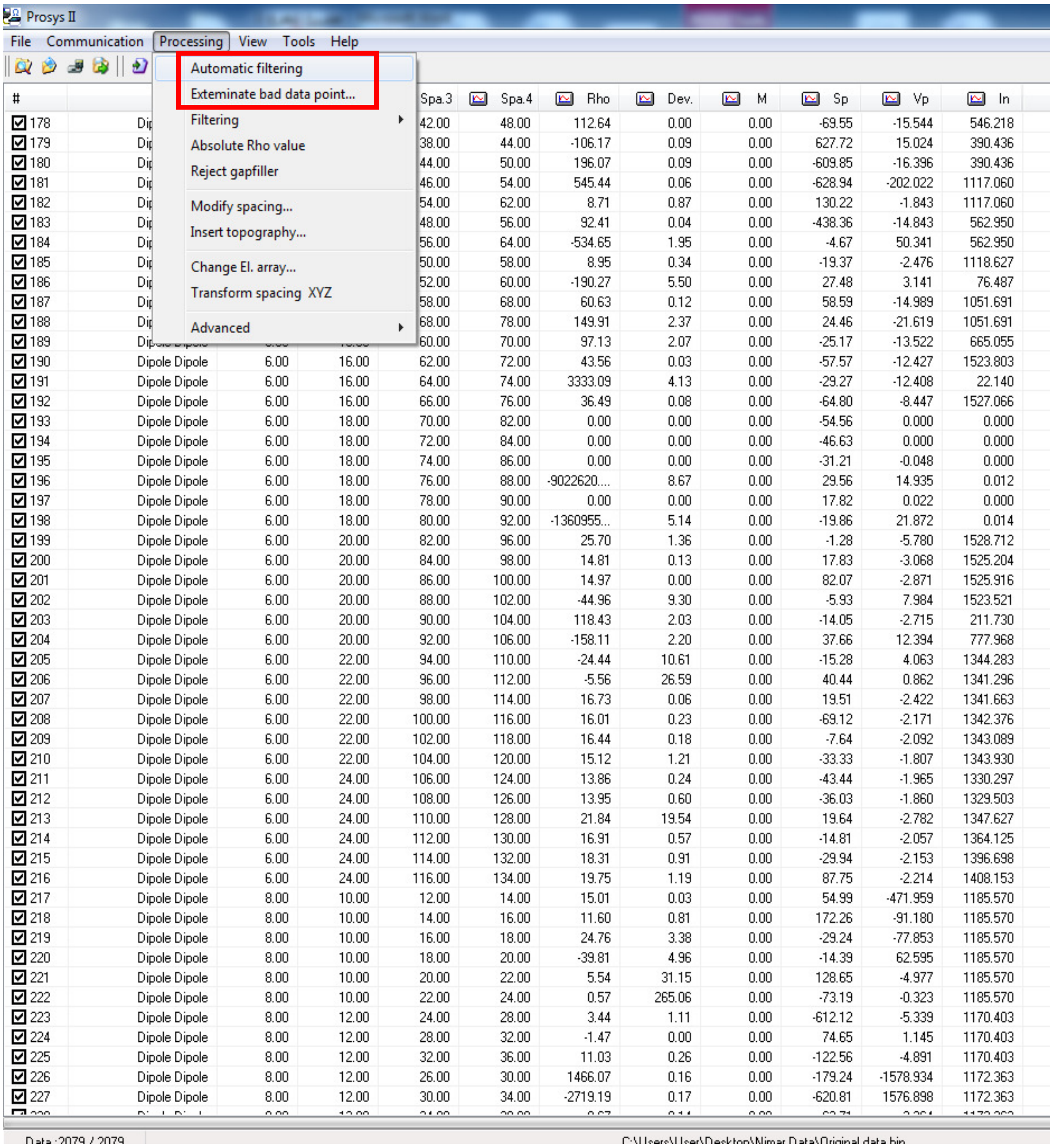

#				Spa.3	Spa.4	Rho	Dev.	M	Sp	Vp	In
178	Di			42.00	48.00	112.64	0.00	0.00	-69.55	-15.544	546.218
179	Di			38.00	44.00	-106.17	0.09	0.00	627.72	15.024	390.436
180	Di			44.00	50.00	196.07	0.09	0.00	-609.85	-16.396	390.436
181	Di			46.00	54.00	545.44	0.06	0.00	-628.94	-202.022	1117.060
182	Di			54.00	62.00	8.71	0.87	0.00	130.22	-1.843	1117.060
183	Di			48.00	56.00	92.41	0.04	0.00	-438.36	-14.843	562.950
184	Di			56.00	64.00	-534.65	1.95	0.00	-4.67	50.341	562.950
185	Di			50.00	58.00	8.95	0.34	0.00	-19.37	-2.476	1118.627
186	Di			52.00	60.00	-190.27	5.50	0.00	27.48	3.141	76.487
187	Di			58.00	68.00	60.63	0.12	0.00	58.59	-14.989	1051.691
188	Di			68.00	78.00	149.91	2.37	0.00	24.46	-21.619	1051.691
189	Di			60.00	70.00	97.13	2.07	0.00	-25.17	-13.522	665.055
190	Dipole Dipole	6.00	16.00	62.00	72.00	43.56	0.03	0.00	-57.57	-12.427	1523.803
191	Dipole Dipole	6.00	16.00	64.00	74.00	3333.09	4.13	0.00	-29.27	-12.408	22.140
192	Dipole Dipole	6.00	16.00	66.00	76.00	36.49	0.08	0.00	-64.80	-8.447	1527.066
193	Dipole Dipole	6.00	18.00	70.00	82.00	0.00	0.00	0.00	-54.56	0.000	0.000
194	Dipole Dipole	6.00	18.00	72.00	84.00	0.00	0.00	0.00	-46.63	0.000	0.000
195	Dipole Dipole	6.00	18.00	74.00	86.00	0.00	0.00	0.00	-31.21	-0.048	0.000
196	Dipole Dipole	6.00	18.00	76.00	88.00	-9022620....	8.67	0.00	29.56	14.935	0.012
197	Dipole Dipole	6.00	18.00	78.00	90.00	0.00	0.00	0.00	17.82	0.022	0.000
198	Dipole Dipole	6.00	18.00	80.00	92.00	-1360955...	5.14	0.00	-19.86	21.872	0.014
199	Dipole Dipole	6.00	20.00	82.00	96.00	25.70	1.36	0.00	-1.28	-5.780	1528.712
200	Dipole Dipole	6.00	20.00	84.00	98.00	14.81	0.13	0.00	17.83	-3.068	1525.204
201	Dipole Dipole	6.00	20.00	86.00	100.00	14.97	0.00	0.00	82.07	-2.871	1525.916
202	Dipole Dipole	6.00	20.00	88.00	102.00	-44.96	9.30	0.00	-5.93	7.984	1523.521
203	Dipole Dipole	6.00	20.00	90.00	104.00	118.43	2.03	0.00	-14.05	-2.715	211.730
204	Dipole Dipole	6.00	20.00	92.00	106.00	-158.11	2.20	0.00	37.66	12.394	777.968
205	Dipole Dipole	6.00	22.00	94.00	110.00	-24.44	10.61	0.00	-15.28	4.063	1344.283
206	Dipole Dipole	6.00	22.00	96.00	112.00	-5.56	26.59	0.00	40.44	0.862	1341.296
207	Dipole Dipole	6.00	22.00	98.00	114.00	16.73	0.06	0.00	19.51	-2.422	1341.663
208	Dipole Dipole	6.00	22.00	100.00	116.00	16.01	0.23	0.00	-69.12	-2.171	1342.376
209	Dipole Dipole	6.00	22.00	102.00	118.00	16.44	0.18	0.00	-7.64	-2.092	1343.089
210	Dipole Dipole	6.00	22.00	104.00	120.00	15.12	1.21	0.00	-33.33	-1.807	1343.930
211	Dipole Dipole	6.00	24.00	106.00	124.00	13.86	0.24	0.00	-43.44	-1.965	1330.297
212	Dipole Dipole	6.00	24.00	108.00	126.00	13.95	0.60	0.00	-36.03	-1.860	1329.503
213	Dipole Dipole	6.00	24.00	110.00	128.00	21.84	19.54	0.00	19.64	-2.782	1347.627
214	Dipole Dipole	6.00	24.00	112.00	130.00	16.91	0.57	0.00	-14.81	-2.057	1364.125
215	Dipole Dipole	6.00	24.00	114.00	132.00	18.31	0.91	0.00	-29.94	-2.153	1396.698
216	Dipole Dipole	6.00	24.00	116.00	134.00	19.75	1.19	0.00	87.75	-2.214	1408.153
217	Dipole Dipole	8.00	10.00	12.00	14.00	15.01	0.03	0.00	54.99	-471.959	1185.570
218	Dipole Dipole	8.00	10.00	14.00	16.00	11.60	0.81	0.00	172.26	-91.180	1185.570
219	Dipole Dipole	8.00	10.00	16.00	18.00	24.76	3.38	0.00	-29.24	-77.853	1185.570
220	Dipole Dipole	8.00	10.00	18.00	20.00	-39.81	4.96	0.00	-14.39	62.595	1185.570
221	Dipole Dipole	8.00	10.00	20.00	22.00	5.54	31.15	0.00	128.65	-4.977	1185.570
222	Dipole Dipole	8.00	10.00	22.00	24.00	0.57	265.06	0.00	-73.19	-0.323	1185.570
223	Dipole Dipole	8.00	12.00	24.00	28.00	3.44	1.11	0.00	-612.12	-5.339	1170.403
224	Dipole Dipole	8.00	12.00	28.00	32.00	-1.47	0.00	0.00	74.65	1.145	1170.403
225	Dipole Dipole	8.00	12.00	32.00	36.00	11.03	0.26	0.00	-122.56	-4.891	1170.403
226	Dipole Dipole	8.00	12.00	26.00	30.00	1466.07	0.16	0.00	-179.24	-1578.934	1172.363
227	Dipole Dipole	8.00	12.00	30.00	34.00	-2719.19	0.17	0.00	-620.81	1576.898	1172.363

Figure (7): Automatic filtering to eliminate zero and enormous resistivity values

Prosys II

File Communication Processing View Tools Help

#	El-array	Spa.1	Spa.2	Spa.3	Spa.4	Rho	Dev.	M	Sp	Vp	In
178	Dipole Dipole	6.00	12.00	42.00	48.00	112.64	0.00	0.00	-69.55	-15.544	546.218
179	Dipole Dipole	6.00	12.00	38.00	44.00	-106.17	0.09	0.00	627.72	15.024	390.436
180	Dipole Dipole	6.00	12.00	44.00	50.00	196.07	0.09	0.00	-609.85	-16.396	390.436
181	Dipole Dipole	6.00	14.00	46.00	54.00	545.44	0.06	0.00	-628.94	-202.022	1117.060
182	Dipole Dipole	6.00	14.00	54.00	62.00	8.71	0.87	0.00	130.22	-1.843	1117.060
183	Dipole Dipole	6.00	14.00	48.00	56.00	92.41	0.04	0.00	-438.36	-14.843	562.950
184	Dipole Dipole	6.00	14.00	56.00	64.00	-534.65	1.95	0.00	-4.67	50.341	562.950
185	Dipole Dipole	6.00	14.00	50.00	58.00	8.95	0.34	0.00	-19.37	-2.476	1118.627
186	Dipole Dipole	6.00	14.00	52.00	60.00	-190.27	5.50	0.00	27.48	3.141	76.487
187	Dipole Dipole	6.00	16.00	58.00	68.00	60.63	0.12	0.00	58.59	-14.989	1051.691
188	Dipole Dipole	6.00	16.00	68.00	78.00	149.91	2.37	0.00	24.46	-21.619	1051.691
189	Dipole Dipole	6.00	16.00	60.00	70.00	97.13	2.07	0.00	-25.17	-13.522	665.055
190	Dipole Dipole	6.00	16.00	62.00	72.00	43.56	0.03	0.00	-57.57	-12.427	1523.803
191	Dipole Dipole	6.00	16.00	64.00	74.00	3333.09	4.13	0.00	-29.27	-12.408	22.140
192	Dipole Dipole	6.00	16.00	66.00	76.00	36.49	0.08	0.00	-64.80	-8.447	1527.066
193	Dipole Dipole	6.00	18.00	70.00	82.00	0.00	0.00	0.00	-54.56	0.000	0.000
194	Dipole Dipole	6.00	18.00	72.00	84.00	0.00	0.00	0.00	-46.63	0.000	0.000
195	Dipole Dipole	6.00	18.00	74.00	86.00	0.00	0.00	0.00	-31.21	-0.048	0.000
196	Dipole Dipole	6.00	18.00	76.00	88.00	-9022620....	8.67	0.00	29.56	14.935	0.012
197	Dipole Dipole	6.00	18.00	78.00	90.00	0.00	0.00	0.00	17.82	0.022	0.000
198	Dipole Dipole	6.00	18.00	80.00	92.00	-1360955...	5.14	0.00	-19.86	21.872	0.014
199	Dipole Dipole	6.00	20.00	82.00	96.00	25.70	1.36	0.00	-1.28	-5.780	1528.712
200	Dipole Dipole	6.00	20.00	84.00	98.00	14.81	0.13	0.00	17.83	-3.068	1525.204
201	Dipole Dipole	6.00	20.00	86.00	100.00	14.97	0.00	0.00	82.07	-2.871	1525.916
202	Dipole Dipole	6.00	20.00	88.00	102.00	-44.96	9.30	0.00	-5.93	7.984	1523.521
203	Dipole Dipole	6.00	20.00	90.00	104.00	118.43	2.03	0.00	-14.05	-2.715	211.730
204	Dipole Dipole	6.00	20.00	92.00	106.00	-158.11	2.20	0.00	37.66	12.394	777.968
205	Dipole Dipole	6.00	22.00	94.00	110.00	-24.44	10.61	0.00	-15.28	4.063	1344.283
206	Dipole Dipole	6.00	22.00	96.00	112.00	-5.56	26.59	0.00	40.44	0.862	1341.296
207	Dipole Dipole	6.00	22.00	98.00	114.00	16.73	0.06	0.00	19.51	-2.422	1341.663
208	Dipole Dipole	6.00	22.00	100.00	116.00	16.01	0.23	0.00	-69.12	-2.171	1342.376
209	Dipole Dipole	6.00	22.00	102.00	118.00	16.44	0.18	0.00	-7.64	-2.092	1343.089
210	Dipole Dipole	6.00	22.00	104.00	120.00	15.12	1.21	0.00	-33.33	-1.807	1343.930
211	Dipole Dipole	6.00	24.00	106.00	124.00	13.86	0.24	0.00	-43.44	-1.965	1330.297
212	Dipole Dipole	6.00	24.00	108.00	126.00	13.95	0.60	0.00	-36.03	-1.860	1329.503
213	Dipole Dipole	6.00	24.00	110.00	128.00	21.84	19.54	0.00	19.64	-2.782	1347.627
214	Dipole Dipole	6.00	24.00	112.00	130.00	16.91	0.57	0.00	-14.81	-2.057	1364.125
215	Dipole Dipole	6.00	24.00	114.00	132.00	18.31	0.91	0.00	-29.94	-2.153	1396.698
216	Dipole Dipole	6.00	24.00	116.00	134.00	19.75	1.19	0.00	87.75	-2.214	1408.153
217	Dipole Dipole	8.00	10.00	12.00	14.00	15.01	0.03	0.00	54.99	-471.959	1185.570
218	Dipole Dipole	8.00	10.00	14.00	16.00	11.60	0.81	0.00	172.26	-91.180	1185.570
219	Dipole Dipole	8.00	10.00	16.00	18.00	24.76	3.38	0.00	-29.24	-77.853	1185.570
220	Dipole Dipole	8.00	10.00	18.00	20.00	-39.81	4.96	0.00	-14.39	62.595	1185.570
221	Dipole Dipole	8.00	10.00	20.00	22.00	5.54	31.15	0.00	128.65	-4.977	1185.570
222	Dipole Dipole	8.00	10.00	22.00	24.00	0.57	265.06	0.00	-73.19	-0.323	1185.570
223	Dipole Dipole	8.00	12.00	24.00	28.00	3.44	1.11	0.00	-612.12	-5.339	1170.403
224	Dipole Dipole	8.00	12.00	28.00	32.00	-1.47	0.00	0.00	74.65	1.145	1170.403
225	Dipole Dipole	8.00	12.00	32.00	36.00	11.03	0.26	0.00	-122.56	-4.891	1170.403
226	Dipole Dipole	8.00	12.00	26.00	30.00	1466.07	0.16	0.00	-179.24	-1578.934	1172.363
227	Dipole Dipole	8.00	12.00	30.00	34.00	-2719.19	0.17	0.00	-620.81	1576.898	1172.363
[illegible]	[illegible]	[illegible]	[illegible]	[illegible]	[illegible]	[illegible]	[illegible]	[illegible]	[illegible]	[illegible]	[illegible]

Data :2079 / 2079 C:\Users\User\Desktop\Nimar Data\Original data.bin

Figure (8): Shows zero and enormous resistivity values.

Step (2): Exterminate bad datum points:

In this option, the apparent resistivity data values are displayed in the form of profiles for each data level. You can use the mouse to remove any bad data point. The main purpose of this option is to remove data points that have resistivity values that are clearly wrong. Such bad data points could be due to the failure of the relays at one of the electrodes, poor electrode ground contact due to dry soil, or shorting across the cables due to very wet ground conditions. These bad data points usually have apparent resistivity values that are obviously too large or too small compared to the neighboring data points. The best way to handle such bad points is to drop them so that they do not influence the model obtained. Figure (4) shows an example of a data set with a few bad points.

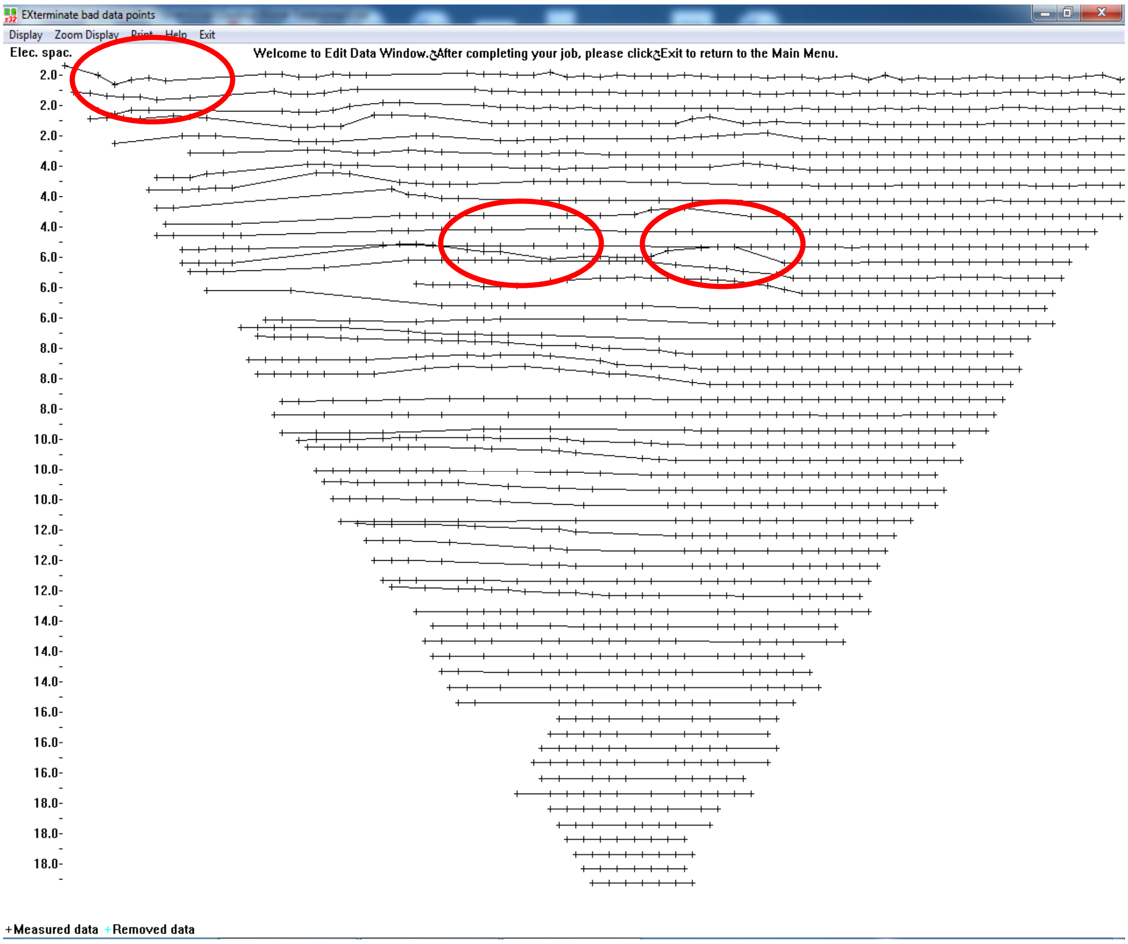

Figure (9): Exterminate bad datum points

Step (3): Exporting the corrected data into RES2DINV format:

This step is important for the coming data inversion, building pseudo sections and interpretation.

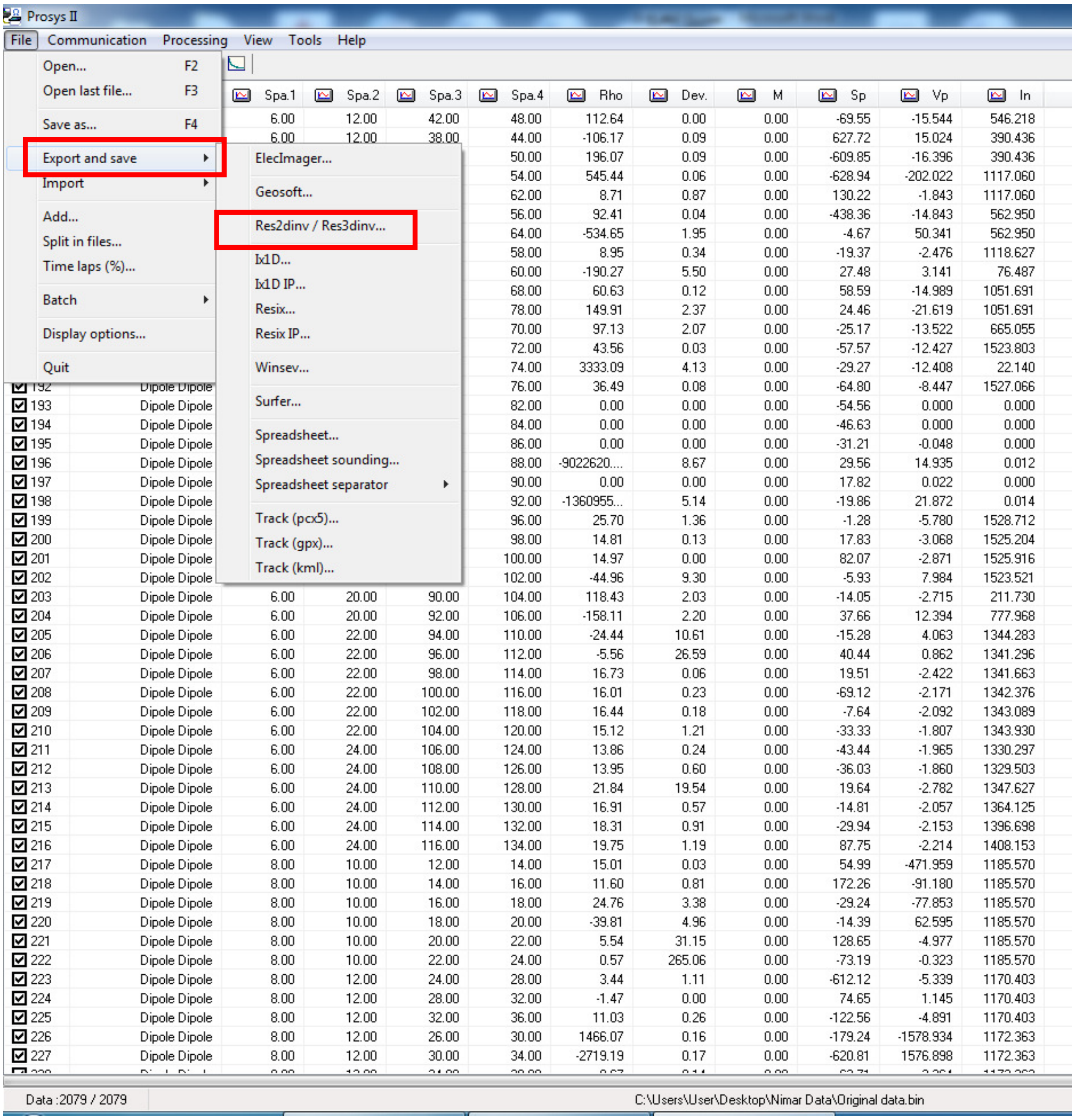

Figure (10): Exporting the corrected data into RES2DINV format.

Results and discussion:

In this study the Syscal Pro was used to acquire a 2D resistivity section with a total length of (360) meter. This section (Figure 11) shows heterogeneity in the topmost (15) meters with circular and semi-circular high resistive anomalies. These types of high resistive anomalies could be interpreted as voids or sinkholes filled with air. This zone is underlain by semi-circular anomalies with low resistivities that extends along the section and directly underlain the above high resistive anomalies. These anomalies that show relatively low resistivities are interpreted as cavities or sinkholes filled with wet clayey sediments.

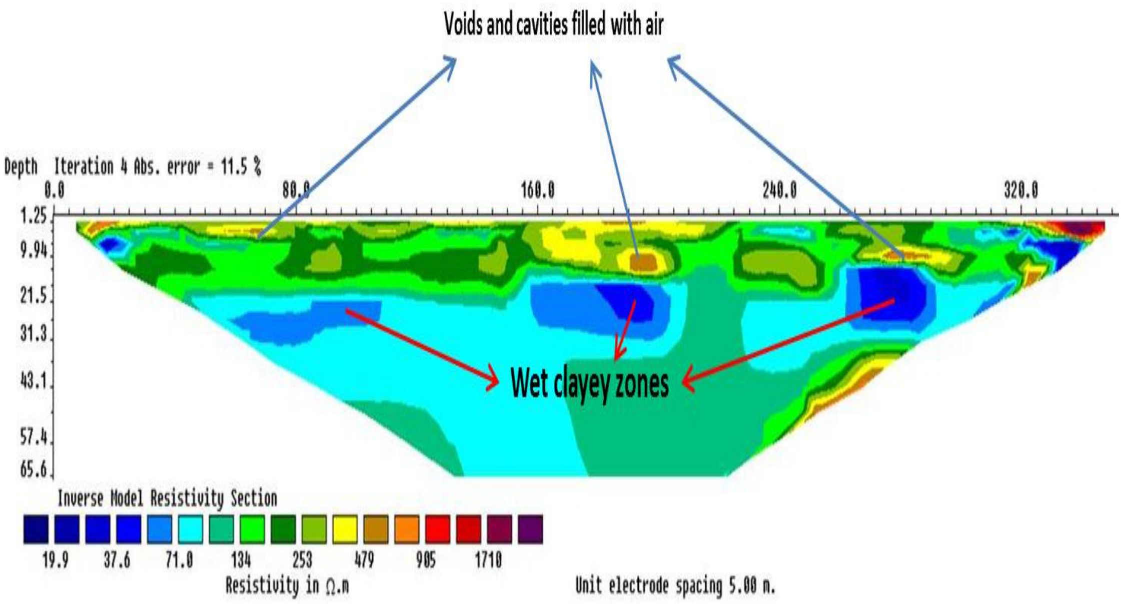

Figure (11): 2D resistivity section for the study area.

REFERENCES

Rene PUTISKA, Maros NIKOLAJ, Ivan DOSTAL, David KUSNIRAK (2012). Determination of cavities using electrical resistivity tomography, Contributions to Geophysics and Geodesy, 201-211.

J. Martı´nez-Lo´pez, J. Rey, J. Duen˜as, C. Hidalgo, and J. Benavente (2013). Electrical tomography applied to the detection of subsurface cavities. Journal of Cave and Karst Studies, 28–37.

Grey I. Riddle, Craig J. Riddle, Douglas R. Schmitt. (2010), ERT and Seismic Tomography in Identifying Subsurface Cavities, AAPG Search and Discovery Article, 1-4

Muhammad Farooq., Samgyu Park., Young Soo Song., Jung Ho Kim., Mohammad Tariq., Adepelumi Adekunle Abraham. (2012), Subsurface cavity detection in a karst environment using electrical resistivity (er): a case study from yongweol-ri, South Korea, EARTH SCIENCES RESEARCH JOURNAL, 75 - 82